Pramana – J. Phys. (2021) 95:92
https://doi.org/10.1007/s12043-021-02086-0

Mathematical modelling of induced magnetisation @ Mn(II) ion doped in perovskite host

MITESH CHAKRABORTY*, SWARAT CHAUDHURI and ARUNAVA MUKHERJEE

Department of Physics, St. Xavier's College, Ranchi 834 001, India
*Corresponding author. E-mail: mitesh.chakraborty@rediffmail.com

MS received 8 May 2020; revised 27 October 2020; accepted 1 December 2020

Abstract. In the present study, zero field splitting (ZFS) parameters are investigated for Mn(II) ion doped perovskites, viz. $PbTiO_3$, $BaTiO_3$ and $SrTiO_3$. The ZFS parameter and magnetisation induced in the host are investigated using quantum mechanical perturbation theory and classical statistics. A mathematical derivation is proposed to study magnetisation and ZFS due to charge distribution generated electric field and spin–orbit coupling (SOC). The computation of ZFS parameters is performed using non-hybrid functional unrestricted Kohn–Sham (UKS). The mathematical formulation is valid for perovskites in the non-ferroelectric state and finite temperature range. The contour plot and mesh surface of the spin–orbit interaction and induced magnetisation are reported.

Keywords. Electron magnetic resonance; zero field splitting; axial symmetry; magnetisation.

PACS Nos 31.5.-p; 71.20.Be; 71.20.Eh; 75.30.Gw

1. Introduction

Transition metal oxides with ABO_3-type perovskite structure have attracted a great deal of research due to their wide range of properties and applications. Perovskites have high superconductivity, colossal magnetoresistance, giant dielectric constant, ferroelectricity, ferroelasticity, ferromagnetism, multiferroicity, optical properties, catalytic activity etc. [1–6]. In electron magnetic resonance (EMR) technology, because of its sensitivity to the local environment, the study of zero field splitting (ZFS) has received considerable attention from theorists and empiricists [7–14]. ZFS parameters are intensively studied by researchers to develop quantum computing, magnetic refrigeration and high memory information system [15–17]. The effect of spin–orbit interaction and covalency makes the distribution of charge about the central metal ion spheroidal and not spherical. This asymmetry is tied to the direction of the spin, so that the rotation of the spin direction relative to the crystal axes changes the exchange energy and also affects the electrostatic interaction energy of the charge distribution on the symmetry of the system [18]. Schlaak and Weiss [19] determined axial ZFS parameter (D) for Mn(II) ion doped in $CdGa_2Se_4$ from EMR study and concluded that strong covalent bonding in Mn–Se bond was responsible for large value of D in selenide. One of the largest value of D is reported for Mn(II) ion doped in $MgTe_2$ where covalent bonding is exceptionally substantial [20]. Watanabe [21] has reported admixture of the ground state with excited state through spin–orbit coupling (SOC) interaction. The Blume-Orbach mechanism considered first-order matrix elements of the axial and rhombic fields between excited quartet states which have been admixed with the ground state through spin–orbit coupling [22]. Studies on ZFS parameters for transition metal ions doped in the host have been done using EMR techniques [23–27]. Chakraborty *et al* [28] have reported the theoretical study of ZFS of Mn(II) ion doped in $KH_3(SeO_3)_2$ single crystal. The contribution of SOC was taken into account. The approach of coupled-perturbed (CP) method was found to be more appropriate than Pederson–Khanna (PK) method in the evaluation of ZFS parameters [28]. In another study of ZFS parameters of Mn(II) ion doped in diaquamalonatozinc(II) single crystal, the unrestricted Kohn–Sham (UKS) orbitals-based PK method as the unperturbed wave function was observed to be suitable for the computational calculation of spin–orbit tensor of the axial ZFS parameter (D). The effect of spin–spin dipolar couplings was also taken into consideration [29]. In both these studies, the theoretical results were in agreement with the experimental observation. The computations were in the distorted octahedronof Mn(II) ion with six

Published online: 27 May 2021

oxygen anions at the interstitial site of the host. The study of magnetisation factor to improve the properties of materials has become an active part of investigation to researchers [30–34]. Magnetisation induced in the host may be due to orbital and/or spin motion of the Fermi electrons [35–39]. Though study of magnetisation from density functional theory has become state of the art, evaluation of magnetisation employing quantum mechanical tools of harmonic oscillator incorporating anharmonic factors is a new beginning [40,41].

In the present paper, axial ZFS parameter (D) and rhombic ZFS parameter (E) are theoretically investigated for Mn(II) ion-doped perovskites, i.e. $PbTiO_3$, $BaTiO_3$ and $SrTiO_3$. The ZFS parameter and magnetisation induced in the host are investigated using quantum mechanical perturbation theory and classical statistics. A mathematical expression is formulated to study magnetisation induced in the host and ZFS due to electron density distribution between Mn(II) and oxygen anions. In the lines of Slater and Barrett, the present paper is confined to the fact that for ABO_3 perovskite systems the 'B' cation acts as an independent harmonic oscillator with small additional harmonic terms. The mathematical study is valid for perovskites in the non-ferroelectric state and finite temperature range. This study is valid in that range of temperature where the chemical interaction of 'A' site cation with 'B' site is insignificant. Previously, Barrett and Slater have imposed this methodology to derive dielectric constants of some perovskites, viz. $BaTiO_3$, $SrTiO_3$, $KTaO_3$ etc. [4,42,43]. The perturbation effect of SOC is also studied in the present investigation. The computational program of ORCA is used to compute the ZFS parameters [44,45]. The computation of ZFS parameters is performed using non-hybrid functional UKS.

2. Quantum mechanical derivation

2.1 *Slater and Barrett theory*

Following Barrett and Slater [42,43]

$$\phi = \phi_{\text{anharmonic terms}} + \lambda \vec{L} \cdot \vec{S}. \tag{1}$$

In the above expression the term consisting of anharmonic factors are related to covalency of the dn ion with the nearest-neighbour interacting atoms. If the covalency in the bonding between the dn ion with the ligands is more, the anharmonic factors will dominate, where

$$\phi_{\text{anharmonic terms}} = a_1\left(x^4 + y^4 + z^4\right) + a_2\left(x^2y^2 + y^2z^2 + z^2x^2\right). \tag{2}$$

a_1 and a_2 are anharmonic terms which depend upon the ionic polarisability of the medium.

Let

$$x' = x - \frac{qE_x}{mw^2}, \quad y' = y - \frac{qE_y}{mw^2}, \quad z' = z - \frac{qE_z}{mw^2}. \tag{3}$$

Using operator tools of the harmonic oscillator

$$\langle x\rangle = \langle n\,|x|\,n\rangle = 0,$$
$$\left\langle x^2\right\rangle = \left\langle n\,\left|x^2\right|\,n\right\rangle = mw\left(n + \frac{1}{2}\right),$$
$$\left\langle n\,\left|x^3\right|\,n\right\rangle = 0. \tag{4}$$

For the symmetrical distribution of unperturbed energy, the contribution is only from diagonal elements. For the execution of the electric field along the three directions, the expression for energy in view of eqs (1)–(3) is as follows:

$$\varepsilon = \mathrm{Tr}\,\langle lmn\,|\phi_{\text{anharmonic terms}}|\,lmn\rangle \tag{5}$$

$$\begin{aligned}\varepsilon = a_1 &\left\{\frac{3}{4\beta^2}[(2l^2+2l+1)\right.\\ &+(2m^2+2m+1)+(2n^2+2n+1)]\\ &+\frac{3q^2}{4a^2\beta}[(2l+1)E_x^2+(2m+1)E_y^2+(2n+1)E_z^2]\\ &\left.+\frac{q^4}{16a^4}[E_x^4+E_y^4+E_z^4]\right\}\\ &+a_2\left\{\frac{1}{4\beta^2}[(2l+1)(2m+1)\right.\\ &+(2l+1)(2n+1)+(2m+1)(2n+1)]\\ &+\frac{q^2}{8a^2\beta}[(2l+1)(E_y^2+E_z^2)+(2m+1)(E_x^2+E_z^2)\\ &+(2n+1)(E_y^2+E_x^2)]\\ &\left.+\frac{q^4}{16a^4}[E_x^2E_y^2+E_x^2E_z^2+E_y^2E_z^2]\right\},\end{aligned} \tag{6}$$

where

$$\beta = \frac{2a}{\hbar\, w} \quad \text{and} \quad a = \frac{1}{2}mw^2.$$

For axial symmetry with constant spheroidal energy surface, the energy $E(k)$ is represented by [18]

$$E(k) = \hbar^2\left(\frac{k_x^2+k_y^2}{2m_t^*} + \frac{k_z^2}{2m_l^*}\right), \tag{7}$$

where m_t^* and m_l^* are transverse and longitudinal mass parameters.

The transverse and longitudinal mass parameters have been empirically determined by Naka *et al* by direct measurement using cyclotron resonance conditions [46].

From electromagnetic theory

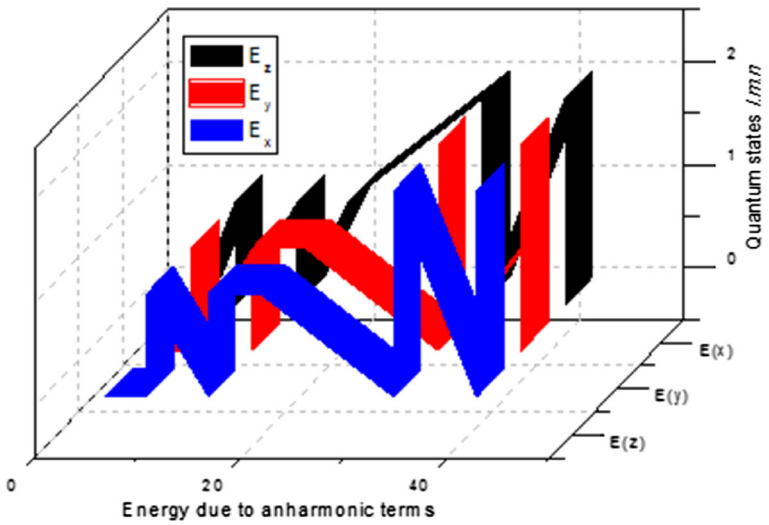

Figure 1. Three-dimensional plot of energy due to anharmonic terms with respect to quantum states l, m and n. The simulation plot is presented for function $\{E(x) = E_z\}$, $\{E(y) = E_y\}$, $\{E(z) = E_x\}$ and quantum states l, m and n.

$$E_i = (v_g)_i B_i \tag{8}$$

$$(v_g)_i = \left(\frac{\partial E}{\partial k_i}\right), \quad i = x, y, z. \tag{9}$$

From eqs (8) and (9), we get [47]

$$(v_g)_x = \frac{k_x}{m_t}, \quad (v_g)_y = \frac{k_y}{m_t}, \quad (v_g)_z = \frac{k_z}{m_l}. \tag{10}$$

Substituting eq. (9) in (7), we get

$$E_x = \frac{k_x}{m_t} B_x, \quad E_y = \frac{k_y}{m_t} B_y, \quad E_z = \frac{k_z}{m_l} B_z. \tag{11}$$

Substituting the expressions for electric field in eq. (4), we get

$$\begin{aligned}
\varepsilon = a_1 \Bigg\{ & \frac{3}{4\beta^2} \Big[(2l^2 + 2l + 1) + (2m^2 + 2m + 1) \\
& + (2n^2 + 2n + 1) \Big] + \frac{3q^2}{4a^2\beta} \Bigg[(2l + 1) \frac{k_x^2 B_x^2}{m_t^2} \\
& + (2m + 1) \frac{k_y^2 B_y^2}{m_t^2} + (2n + 1) \frac{k_z^2 B_z^2}{m_l^2} \Bigg] \\
& + \frac{q^4}{16a^4} \left[\frac{k_x^4 B_x^4}{m_t^4} + \frac{k_y^4 B_y^4}{m_t^4} + \frac{k_z^4 B_z^4}{m_l^4} \right] \Bigg\} \\
& + a_2 \Bigg\{ \frac{1}{4\beta^2} \left[(2l + 1)(2m + 1) + (2l + 1)(2n + 1) \right. \\
& \left. + (2m + 1)(2n + 1) \right] \\
& + \frac{q^2}{8a^2\beta} \Bigg[(2l + 1) \left(\frac{k_y^2 B_y^2}{m_t^2} + \frac{k_z^2 B_z^2}{m_l^2} \right) \\
& + (2m + 1) \left(\frac{k_x^2 B_x^2}{m_t^2} + \frac{k_z^2 B_z^2}{m_l^2} \right) \\
& + (2n + 1) \left(\frac{k_y^2 B_y^2}{m_t^2} + \frac{k_x^2 B_x^2}{m_t^2} \right) \Bigg] + \frac{q^4}{16a^4} \\
& \times \left[\frac{k_x^2 B_x^2}{m_t^2} \cdot \frac{k_y^2 B_y^2}{m_t^2} + \frac{k_x^2 B_x^2}{m_t^2} \cdot \frac{k_z^2 B_z^2}{m_l^2} \right. \\
& \left. + \frac{k_y^2 B_y^2}{m_t^2} \cdot \frac{k_z^2 B_z^2}{m_l^2} \right] \Bigg\}
\end{aligned} \tag{12}$$

$$\begin{aligned}
\varepsilon = a_1 \Bigg\{ & \frac{3}{4\beta^2} \left[(2l^2 + 2l + 1) + (2m^2 + 2m + 1) \right. \\
& \left. + (2n^2 + 2n + 1) \right] \\
& + \frac{3q^2}{4a^2\beta} \Bigg[(2l + 1) \frac{k_x^2 B_x^2}{m_t^2} + (2m + 1) \frac{k_y^2 B_y^2}{m_t^2} \\
& + (2n + 1) \frac{k_z^2 B_z^2}{m_l^2} \Bigg] + \frac{q^4}{16a^4} \left[\frac{k_x^4 B_x^4}{m_t^4} \right. \\
& \left. + \frac{k_y^4 B_y^4}{m_t^4} + \frac{k_z^4 B_z^4}{m_l^4} \right] \Bigg\} \\
& + a_2 \Bigg\{ \frac{1}{4\beta^2} \left[(2l + 1)(2m + 1) + (2l + 1)(2n + 1) \right. \\
& \left. + (2m + 1)(2n + 1) \right] + \frac{q^2}{8a^2\beta} \Bigg[(2l + 1) \left(\frac{k_y^2 B_y^2}{m_t^2} \right. \\
& \left. + \frac{k_z^2 B_z^2}{m_l^2} \right) + (2m + 1) \left(\frac{k_x^2 B_x^2}{m_t^2} + \frac{k_z^2 B_z^2}{m_l^2} \right)
\end{aligned}$$

$$+(2n+1)\left(\frac{k_y^2B_y^2}{m_t^2}+\frac{k_x^2B_x^2}{m_t^2}\right)\Bigg]+\frac{q^4}{16a^4}$$
$$\times\left[\frac{k_x^2B_x^2}{m_t^2}\cdot\frac{k_y^2B_y^2}{m_t^2}+\frac{k_x^2B_x^2}{m_t^2}\cdot\frac{k_z^2B_z^2}{m_l^2}\right.$$
$$\left.+\frac{k_y^2B_y^2}{m_t^2}\cdot\frac{k_z^2B_z^2}{m_l^2}\right]\Bigg\} \tag{13}$$

where

$$\beta=\frac{2a}{\hbar w}\text{ and }a=\frac{1}{2}mw^2.$$

2.2 *Magnetisation through effective perturbation*

In a magnetic solid, the magnetic moment due to each spin moment interacting with the unquenched orbital moment can be mathematically expressed as $\hat{H}_{\text{SOC}}=\lambda\hat{L}\cdot\hat{S}$. The effect of spin–orbit coupling has been considered on the basis of empirical studies. For quantised states, L and S are treated as operators, and for $\vec{L}\rightarrow\hat{L}$ and $\vec{S}\rightarrow\hat{S}$, the contribution from SOC is restricted to second-order correction in energy. The mathematical description is given as follows [48]:

$$H_{\text{SOC}}=H_{\text{SOC}}^1+H_{\text{SOC}}^2. \tag{14}$$

From standard quantum mechanical perturbation formula with second-order correction to energy, SOC is expressed as

$$H_{\text{SOC}}=\left\langle\psi_n^0\middle|\lambda\hat{L}\cdot\hat{S}\middle|\psi_k^0\right\rangle+\frac{\sum_{n,n\neq k}\left\langle\psi_n^0\middle|\lambda\hat{L}\cdot\hat{S}\middle|\psi_k^0\right\rangle^2}{(E_n^0-E_k^0)}. \tag{15}$$

For non-degenerate ground orbital function $\left\langle\psi_0\middle|\hat{L}_\mu\middle|\psi_0\right\rangle=0$ for $\mu=x,y,z$ and $\langle\psi_n\left|\hat{S}\right|\psi_0\rangle=0$ where ψ_n and ψ_0 are the excited state and ground state respectively. The degenerate state of the d-electrons of the dopant Mn(II) ion in the distorted octahedron symmetry splits into five non-degenerate states. The states are represented as $|2,-2\rangle\rightarrow d_{xy}$,$|2,-1\rangle\rightarrow d_{yz}$,$|2,0\rangle\rightarrow d_{zx}$, $|2,+1\rangle\rightarrow d_{z^2}$ and $|2,+2\rangle\rightarrow d_{x^2-y^2}$ with energy eigenvalues E_0, E_1, E_2, E_3 and E_4 respectively. The reference wave function $\left|\psi_n^0\right\rangle$ is the ground state and $\left|\psi_n^0\right\rangle$ states be d_{yz}, d_{zx}, d_{z^2} and $d_{x^2-y^2}$.

$$H_{\text{SOC}}^2=\frac{\sum_{n,n\neq k}\left|\left\langle\psi_n^0\middle|\lambda\hat{L}\cdot\hat{S}\middle|\psi_k^0\right\rangle\right|^2}{(E_n^0-E_k^0)} \tag{16}$$

$$H_{\text{SOC}}^2=\lambda^2\hat{S}_\mu\Lambda_{\mu\upsilon}\hat{S}_\upsilon, \tag{17}$$

where

$$\Lambda_{\mu\upsilon}=\sum_{n=0,k}^{\text{excited states}}\frac{\langle\psi_0\,|\hat{L}_\mu|\,\psi_k\rangle\,\langle\psi_k\,|\hat{L}_\upsilon|\,\psi_0\rangle}{E_k-E_0}, \tag{18}$$

$$\Lambda_{\mu\upsilon}=0,\text{ when }\quad\mu\neq\upsilon. \tag{19}$$

The factor $\Lambda_{\mu\upsilon}$ of eq. (18) for $\mu\upsilon=xx,yy,zz$ is calculated and presented in tabular form in tables 1, 2 and 3 respectively. $\Lambda_{\mu\upsilon}$ is evaluated using the operator algebra. The equation is given in Appendix A.

From eqs (11) and (15), the ZFS term is presented in the form

$$D\hat{S}_z^2=\varepsilon+H_{\text{SOC}}^2. \tag{20}$$

Following classical statistics, the distribution function is expressed as

$$Z=\sum_i \mathrm{e}^{-\beta E_i}.$$

The free energy of the system is given by $F=-k_BT\log Z$. Let z be the partition function of a single oscillator and $z^N/N!$ be the partition function of N such oscillators [42,49]. The partition function of the system is given by $w=z^N/N!$.

Taking logarithms on both the sides of the equation

$$\ln w=N\ln z-\ln N! \tag{21}$$

with Stirling approximation

$$\ln w=N\ln(\sum_i \mathrm{e}^{-\beta\varepsilon_i})-(N\ln N-N). \tag{22}$$

Let

$$x=\sum_i \mathrm{e}^{-\beta\varepsilon_i}, \tag{23}$$

where

$$\varepsilon_i=\varepsilon+H_{\text{SOC}}^2, \tag{24}$$

Then, $\ln w=N\ln(1-x)-(N\ln N-N)$. Further $\ln(1-x)=-x$. This approximation is justified on the basis of assuming small perturbation from anharmonic terms.

The free energy of the system is given by

$$F=-k_BT\log w \tag{25}$$

$$F=-k_BT[-Nx-(N\ln N-N)]. \tag{26}$$

The spontaneous induced magnetisation is expressed by

$$M_i=-\left(\frac{\partial F}{\partial B_i}\right),\quad i=x,y,z. \tag{27}$$

The magnetisation developed in the system due to the induced electric field contributes to ZFS and hence should be taken into account.

The induced magnetisation along the z-direction is given by

$$M_Z = Nk_BT\frac{\partial x}{\partial B_z}. \tag{28}$$

From eqs (11), (15) and (19)

$$\begin{aligned} k_BT\cdot\frac{\partial x}{\partial B_Z} &= a_1\left\{\frac{3q^2}{4a^2\beta}(2n+1)\frac{k_z^2}{m_l^2}2B_z+\frac{q^4}{16a^4}\frac{k_z^4}{m_l^4}4B_z^3\right\}\\ &+a_2\left\{\begin{array}{l}\frac{q^2}{8a^2\beta}[(2l+1)+(2m+1)]\frac{k_z^2}{m_l^2}2B_z\\ +\frac{q^4}{16a^4}\left[\frac{k_x^2B_x^2}{m_t^2}+\frac{k_y^2B_y^2}{m_t^2}\right]\frac{k_z^2 2B_z}{m_l^2}\end{array}\right\}+\frac{\partial H_{\mathrm{SOC}}^2}{\partial B_z} \end{aligned} \tag{29}$$

$$M_z = N\left\{\begin{array}{l} a_1\left\{\frac{3q^2}{4a^2\beta}(2n+1)\frac{k_z^2}{m_l^2}2B_z+\frac{q^4}{16a^4}\frac{k_z^4}{m_l^4}4B_z^3\right\}\\ +a_2\left\{\begin{array}{l}\frac{q^2}{8a^2\beta}[(2l+1)+(2m+1)]\frac{k_z^2}{m_l^2}2B_z\\ +\frac{q^4}{16a^4}\left[\frac{k_x^2B_x^2}{m_t^2}+\frac{k_y^2B_y^2}{m_t^2}\right]\frac{k_z^2 2B_z}{m_l^2}\end{array}\right\}+\frac{\partial H_{\mathrm{SOC}}^2}{\partial B_z}\end{array}\right\}. \tag{30}$$

If the system is axially symmetric and the transverse mass parameter is constant in the X–Y plane, we assume $B_x = B_y$ and $k_x = k_y$ in eq. (21), and the net effective magnetisation can be expressed as

$$\begin{aligned} M_z' &= a_1\left\{\frac{3q^2}{4a^2\beta}(2n+1)\frac{k_z^2}{m_l^2}2B_z+\frac{q^4}{16a^4}\frac{k_z^4}{m_l^4}4B_z^3\right\}\\ &+a_2\left\{\begin{array}{l}\frac{q^2}{8a^2\beta}[(2l+1)+(2m+1)]\frac{k_z^2}{m_l^2}2B_z\\ +\frac{q^4}{16a^4}\frac{2k_x^2B_x^2}{m_t^2}\frac{k_z^2 2B_z}{m_l^2}\end{array}\right\}\\ &+\nabla_{B_z}H_{\mathrm{SOC}}^2 \end{aligned} \tag{31}$$

Table 1. Calculation of $\Lambda_{\mu\nu}$ for $\mu = \nu = x$ for Mn(II) ion at the interstitial site of the perovskite host.

Quantum states	$\|2,-2\rangle$	$\|2,-1\rangle$	$\|2,0\rangle$	$\|2,+1\rangle$	$\|2,+2\rangle$
$\|2,-2\rangle$	0	$\frac{1}{E_1-E_0}$	0	0	0
$\|2,-1\rangle$	$\frac{1}{E_0-E_1}$	0	$\frac{(\sqrt{6}/2)^2}{E_2-E_1}$	0	0
$\|2,0\rangle$	0	$\frac{(\sqrt{6}/2)^2}{E_1-E_2}$	0	$\frac{(\sqrt{6}/2)^2}{E_3-E_2}$	0
$\|2,+1\rangle$	0	0	$\frac{(\sqrt{6}/2)^2}{E_2-E_3}$	0	$\frac{1}{E_4-E_3}$
$\|2,+2\rangle$	0	0	0	$\frac{1}{E_3-E_4}$	0

Table 2. Calculation of $\Lambda_{\mu\nu}$ for $\mu = \nu = y$ for Mn(II) ion at the interstitial site of the perovskite host.

Quantum states	$\|2,-2\rangle$	$\|2,-1\rangle$	$\|2,0\rangle$	$\|2,+1\rangle$	$\|2,+2\rangle$
$\|2,-2\rangle$	0	$\frac{1}{E_0-E_1}$	0	0	0
$\|2,-1\rangle$	$\frac{1}{E_1-E_0}$	0	$\frac{(\sqrt{6}/2i)^2}{E_2-E_1}$	0	0
$\|2,0\rangle$	0	$\frac{(\sqrt{6}/2i)^2}{E_1-E_2}$	0	$\frac{(\sqrt{6}/2i)^2}{E_3-E_2}$	0
$\|2,+1\rangle$	0	0	$\frac{(\sqrt{6}/2i)^2}{E_2-E_3}$	0	$\frac{1}{E_3-E_4}$
$\|2,+2\rangle$	0	0	0	$\frac{1}{E_4-E_3}$	0

Table 3. Calculation of $\Lambda_{\mu\nu}$ for $\mu = \nu = z$ for Mn(II) ion at the interstitial site of the perovskite host.

Quantum states	$\|2,-2\rangle$	$\|2,-1\rangle$	$\|2,0\rangle$	$\|2,+1\rangle$	$\|2,+2\rangle$
$\|2,-2\rangle$	-2	0	0	0	0
$\|2,-1\rangle$	0	-1	0	0	0
$\|2,0\rangle$	0	0	0	0	0
$\|2,+1\rangle$	0	0	0	$+1$	0
$\|2,+2\rangle$	0	0	0	0	$+2$

$$H^2_{\mathrm{SOC}} = \lambda^2\left[\lambda_{xx}s_x^2 + \lambda_{yy}s_y^2 + \lambda_{zz}s_z^2\right]$$

$$\frac{\partial H^2_{\mathrm{SOC}}}{\partial B_z} = 2\lambda^2 \times\left[\lambda_{xx}s_x\frac{\partial s_x}{\partial B_z} + \lambda_{yy}s_y\frac{\partial s_y}{\partial B_z} + \lambda_{zz}s_z\frac{\partial s_z}{\partial B_z}\right] \tag{32}$$

$$s_x \to f\,(E,\ B_x)\,,\ s_y \to f\left(E,\ B_y\right),\ s_z \to f\,(E,\ B_z)$$

$$s_x = K\left[f\,(E,B_x)_{l,m,n=0} + \sum_{l,m,n=0}\frac{\partial f\,(E)_{l,m,n}}{\partial B_z} + \sum_{l,m,n=0}\frac{\partial^2 f(E)_{l,m,n}}{\partial B_z^2} + \cdots\right] \tag{33a}$$

$$s_y = K\left[f\left(E,B_y\right)_{l,m,n=0} + \sum_{l,m,n=0}\frac{\partial f\,(E)_{l,m,n}}{\partial B_z} + \sum_{l,m,n=0}\frac{\partial^2 f(E)_{l,m,n}}{\partial B_z^2} + \cdots\right] \tag{33b}$$

$$s_z = K\left[f\,(E,B_z)_{l,m,n=0} + \sum_{l,m,n=0}\frac{\partial f\,(E,\ B_z)_{l,m,n=0}}{\partial B_z} + \sum_{l,m,n=0}\frac{\partial^2 f(E,\ B_z)_{l,m,n}}{\partial B_z^2} + \cdots\right]. \tag{33c}$$

The constant factor K depends upon the Bohr magneton.

3. Computational details

The contour molecular orbital plots and mesh surface of Mn(II) ion in the distorted octahedron with oxygen anions for spin contributions s_x, s_y and s_z are presented. The computational study is performed using ORCA [44,45]. The non-hybrid functional UKS is reported in the present investigation. The auxiliary basis set Kahlsruhe polarised TPSS, def2-TZVP/J and def2-TZVP/j ZORA have been employed for the calculations. In the present calculation, the perturbation effect of SOC has been represented by the spin–orbit mean-field (SOMF) method [50–52]. The COSMO model is used for dielectric modelling of the environment. The SOC calculation is performed by coupled-perturbed (CP) and Pederson–Khanna (PK) [53,54] methods.

3.1 *Results and discussion*

The magnitude of the D-tensor evaluated for non-hybrid functional UKS for Mn(II) ion doped in different perovskite hosts, viz. $PbTiO_3$, $BaTiO_3$ and $SrTiO_3$, is reported in the present investigation. The principal values of the axial ZFS parameter D is presented in table 4.

Table 4. The axial ZFS parameter D and rhombic ZFS parameter E evaluated for Mn(II) ion doped in different perovskite hosts.

Unrestricted Kohn Sahm (UKS) ZFS parameters (10^{-4} cm^{-1})				
TZVP/TZVP/J/ZORA	CP		PK	
ZFS parameters	D	E	D	E
Mn^{2+}: $PbTiO_3$	102.3	18.41	151.1	27.20
Mn^{2+}: $BaTiO_3$	77.8	12.44	107.7	18.31
Mn^{2+}: $SrTiO_3$	62.4	9.36	81.3	11.38

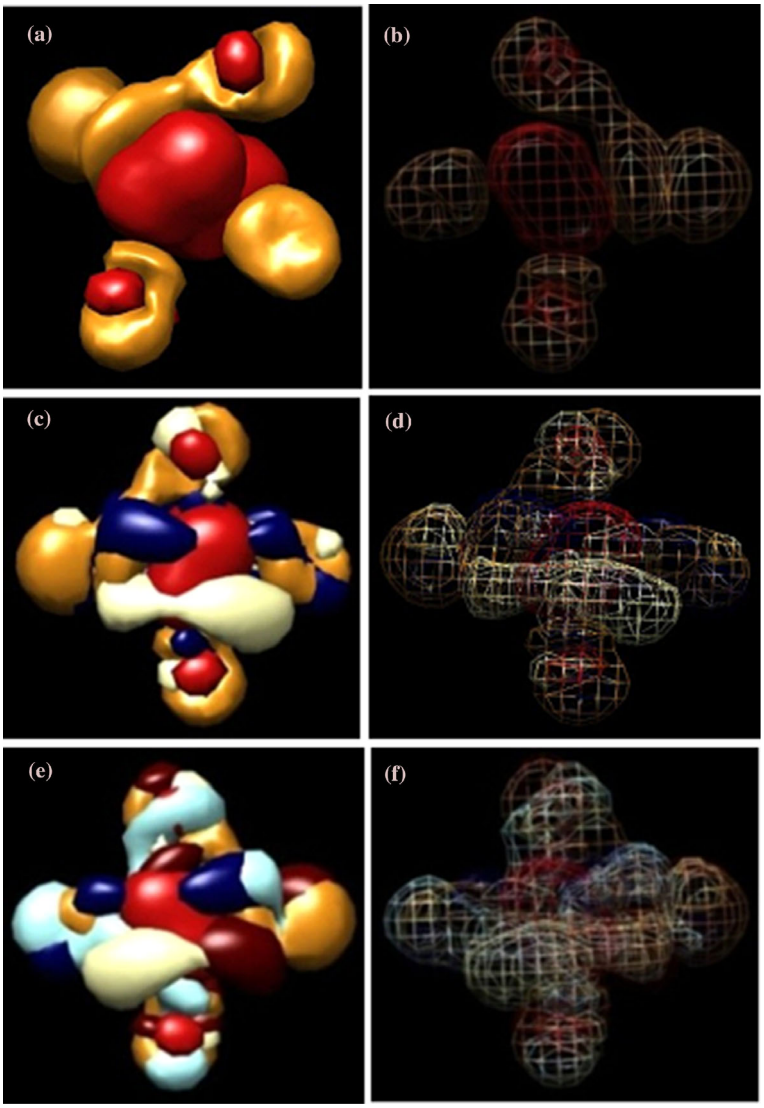

Figure 2. Contour plot representation of spin–orbit interaction for Fermi electron state $d_{x^2-y^2}$ of the dopant Mn(II) ion in the perovskite host with effective contribution from (**a**) s_x, (**c**) $s_x + s_y$, (**e**) $s_x + s_y + s_z$. Mesh surface representation (**b**) s_x, (**d**) $s_x + s_y$, (**f**) $s_x + s_y + s_z$.

From table 4 it is evident that there is a remarkable difference in the computation of ZFS parameter from the method of CP and PK. All computations are in the distorted octahedron symmetry of Mn(II) ion about the six oxygen anions of the perovskite structure. The difference in the values of D and rhombic ZFS parameter (E) may be due to ionic difference of Pb(II), Sr(II) and Ba(II) ions in the host. It is this difference in ionic radii of the metal ion at the 'A' site of the perovskite structure which exhibits change in symmetry of the base compound. When Mn(II) ion is doped in the host, the Z-matrix accounts for self-consistent field (SCF) convergence with changes in bond length and bond angles between Mn(II) ion and oxygen anions in the distorted octahedron, and this accounts for different ZFS parameters D. The computation of ZFS parameters was also investigated for hybrid functional B3LYP with the basis set TPSSh. But SCF did not converge for hybrid functional B3LYP with the host $PbTiO_3$, $BaTiO_3$ and $SrTiO_3$ as such computation did not yield result of ZFS tensor D. The computation of gyromagnetic ratio (g) for the host with the dopant Mn(II) ion yields $g_{xx} \neq g_{yy} \neq g_{zz}$. For the host $PbTiO_3$, $g_{xx} = 2.0023$, $g_{yy} = 2.0027$ and $g_{zz} = 2.0134$, for $BaTiO_3$, $g_{xx} = 2.0010$, $g_{yy} = 2.00102$ and $g_{zz} = 2.0126$ and for $SrTiO_3$, $g_{xx} = 2.0007$, $g_{yy} = 2.0009$ and $g_{zz} = 2.0021$. From the computation values of g it can be said that the system exhibits axial distortion with rhombic asymmetry.

The contribution of the perturbation effect of spin–orbit interaction (H_{SO}) to magnetisation (M_z') of the d-block Fermi electron $d_{x^2-y^2}$ is represented by contour plot and mesh surface in figure 2. It is evident from

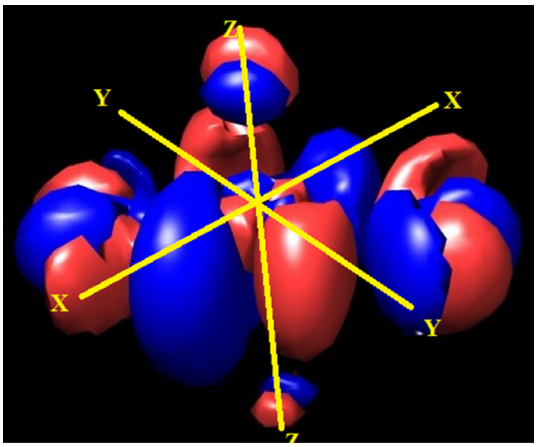

Figure 3. Contour plot of magnetisation (M_z') induced in the Mn(II)-doped perovskite host.

figure 2 that electron density moderately changes from non-uniform distribution for spin projection along x-direction (s_x) to uniformity with effective role of spin projection along y direction (s_y) and z direction (s_z) (figure 2e). The interpretation of eq. (33c) which has additional differentiation terms relative to eqs (12) and (13) is observed in the computational calculations of D and E. The dopant Mn(II) ion at the 'B' site of the perovskite host in the distorted octahedron structure is axially distorted with rhombic asymmetry.

The magnetisation is induced in the system due to the chemical interaction between the d block electrons of the dopant Mn(II) ion with p-block electrons of oxygen anions. It is observed from figure 3 that magnetisation is axially distorted along z-direction. The graphical representations of contour plots and mesh surface in figures 2 and 3 are presented with UCSCF Chimera software [55].

4. Conclusion

The mathematical formulation of D is in agreement with the computational calculation for non-hybrid functional UKS with basis set def2-TZVP, def2-TZVP/jZORA. It is observed from the computation that $g_{xx} \neq g_{yy} \neq g_{zz}$ and hence the system reveals axial distortion with rhombic asymmetry. The effective contribution of electron spin along X, Y and Z directions is presented with contour plots and mesh surface. The mathematical derivation of induced magnetisation M_z' is analysed through molecular orbital interaction of the d electrons of Mn(II) with p electrons of oxygen at the Fermi state. The theoretical study of ZFS and induced magnetisation may improve the synthesis of new materials for developing magnetic refrigerators and molecular magnets.

Acknowledgements

The authors are grateful to the University Grants Commission (UGC), New Delhi, India for providing financial assistance in the form of Colleges with Potential for Excellence (CPE) status to St. Xavier's College, Ranchi, India (DO/21-49/2014/PE).

Appendix A

$$L_+|L, M_L\rangle = \sqrt{(L - M_L)(L + M_L + 1)}|L, M_{L+1}\rangle$$
$$L_-|L, M_L\rangle = \sqrt{(L - M_L)(L + M_L + 1)}|L, M_{L-1}\rangle$$
$$L_z|L, M_L\rangle = M_L|L, M_L\rangle.$$

References

[1] R Wang, M Mujahid, Y Duan, Z K Wang, J Xue and Y Yang, *Adv. Func. Mater.* **29**, 1808843 (2019)
[2] S Yamada, N Abe, H Sagayama, K Ogawa, T Yamagami and T Arima, *Phys. Rev. Lett.* **123**, 126602 (2019)
[3] M Chakraborty, V K Rai and K Mitra, *Pramana – J. Phys.* **92**: 46 (2019)
[4] M Chakraborty, S Chaudhuri, V K Rai and V Mishra, *J. Mater. Sci.: Mater.* **27**, 7478 (2016)
[5] R Kumar, R J Choudhary and S I Patil, *NATO Science Series* **235**, 535 (2007)
[6] S Hikami and Y Matsuda, *Jpn. J. Appl. Phys.* **26**, 26 (1987)
[7] C Duboc, D Ganyushin, K Sivalingam, M Collomb and F Neese, *J. Phys. Chem. A* **114**, 10750 (2010)
[8] M Atanasov and F Neese, *Coordin. Chem. Rev.* **257**, 27 (2013)
[9] R Maurice, R Broer, N Guihery and C Graaf, *Handbook of relativistic quantum chemistry* (Springer, Berlin, 2016)
[10] J A Clayton, K Keller, M Qi, J Wegner, V Koch, H Hintz, A Godt, S Han, G Jeschke, M S Sherwin and M Yulikov, *Phys. Chem. Chem. Phys.* **15**, 1 (2018)
[11] J Lu, I Ozel, C A Belvin, X Li, G Skorupskii, L Sun, O Okai, M Dinca, N Gedik and K A Nelson, *Chem. Sci.* **8**, 7312 (2017)
[12] J Kobak, A Bogucki, T Smolenski, M Papaj, M Kossacki, A Golnik and W Pacuski, *Phys. Rev. B* **97**, 04530 (2018)
[13] M Zajac, C Rudowicz, H Ohta and T Sakurai, *J. Magn. Magn. Mater.* **449**, 94 (2018)
[14] A W Lloyd, H M Moylan and J W McDouall, *Magnetochemistry* **5**, 3 (2019)
[15] D A Garanin and E M Chudnovsky, *Phys. Rev. B* **56**, 11102 (1997)
[16] M N Leuenberger and D Loss, *Nature* **410**, 789 (2001)
[17] S Loth, K Von Bergmann, M Ternes, A F Otte, C P Lutz and A J Heinrich, *Nat. Phys.* **6**, 340 (2010)

[18] C Kittel, *Introduction to solid state physics* (Wiley, New York, 2009)
[19] M Schlaak and A Weiss, *Z. Naturforsch. A* **27**, 1624 (1972)
[20] T Miyadi and O Okada, *Jpn. J. Phys.* **17**, 231 (1978)
[21] H Watanabe, *Prog. Theor. Phys.* **18**, 405 (1957)
[22] M Blume and R Orbach, *Phys. Rev*. **127**, 1587 (1962)
[23] R Kripal and V Mishra, *J. Mag. Res*. **172**, 201 (2005)
[24] R HariKrishna, B M Nagabhushana, H Nagabhushana, D L Monika, R Sivaramakrishna, C Shivakumara, R P S Chakradhar and T Thomas, *J. Lumin*. **155**, 125 (2014)
[25] S K Misra, S I Andronenko, A Thurber, A Punnoose and A Nalepa, *J. Magn. Magn. Mater.* **363**, 82 (2014)
[26] R Kripal, M Maurya and H Govind, *Physica B* **392**, 281 (2007)
[27] R Kripal and S Pandey, *Physica B* **444**, 14 (2014)
[28] M Chakraborty, V K Rai and V Mishra, *Optik* **127**, 4333 (2016)
[29] M Chakraborty and V K Rai, *Pramana – J. Phys*. **89**: 88 (2017)
[30] X Lan, S Kong and W Y Zhang, *Eur. Phys. J. B* **84**, 357 (2011)
[31] A Haque, D Ghosh, U Dutta, A Shukla, A Gayen, P Mahata, A K Kundu and Md Seikh, *J. Magn. Magn. Mater.* **494**, 165847 (2020)
[32] J Meng, L Zhang, F Yao, X Liu, J Meng and H Zhang, *Inorg. Chem*. **56**, 6371 (2017)
[33] I Alkotra and J Elguero, *New J. Chem*. **42**, 13889 (2018)
[34] S Biswas and S Pal, *Rev. Adv. Mater. Sci.* **53**, 206 (2018)
[35] T Thonhauser, *Int. J. Mod. Phys. B* **25**, 1429 (2011)
[36] J Shi, G Vignale and D Xiao, *Phys. Rev. Lett*. **99**, 197202 (2007)
[37] S Acheche, R Nourafkan and A M S Tremblay, *Phys. Rev. B* **99**, 075144 (2019)
[38] T N Ikeda and M Sato, *Phys. Rev. B* **100**, 214424 (2019)
[39] G P Zhang, M S Si, M Murakami, Y H Bai and T F George, *Nat. Commun*. **9**, 3031 (2018)
[40] G Vignale and M Rasolt, *Phys. Rev. B* **37**, 10685 (1988)
[41] G Vignale and M Rasolt, *Phys. Rev. Lett*. **59**, 2360 (1987)
[42] J H Barrett, *Phys. Rev.* **86**, 1 (1952)
[43] J Slater, *Phys. Rev.* **78**, 6 (1950)
[44] F Neese, *ORCA – An Ab Initio, Density Functional and Semiempirical Program Package, version 3.0.3* (Max-Planck-Institute for Chemische Energiekonversion, Germany)
[45] F Neese, *Wiley Interdisciplinary Reviews – Comput. Mol. Sci.* **2**, 73 (2012)
[46] N Naka, K Fukai, Y Handa and I Akimoto, *Phys. Rev. B* **88**, 035205 (2013)
[47] G Dresselhaus, A F Kip and C Kittel, *Phys. Rev*. **98**, 2 (1955)
[48] D Dai, H Xiang and M H Whangbo, *J. Comput. Chem.* **29**, 2187 (2008)
[49] R K Pathria and P D Beale, *Statistical mechanics* (Butterworth-Heinemann, India, 1996)
[50] B A Hess, C M Marian, U Wahlgren and O Gropen, *Chem. Phys. Lett.* **251**, 365 (1996)
[51] A D Becke, *Phys. Rev. A* **38**, 3098 (1988)
[52] S Zein, C Duboc, W Lubitz and F Neese, *Inorg. Chem.* **47**, 134 (2008)
[53] K Sugisaki, K Toyota, K Sato, D Shiomi and T Takui, *Phys. Chem. Chem. Phys*. **19**, 30128 (2017)
[54] R Pederson and S N Khanna, *Phys. Rev. B* **60**, 9566 (1999)
[55] E F Pettersen, T D Goddard, C C Huang, G S Couch, D M Greenblatt, E C Meng and T E Ferrin, *J. Comput. Chem.* **25**, 1605 (2004)